13th National Conference on Mechanisms and Machines (NaCoMM07),
IISc, Bangalore, India, December 12-13, 2007

NaCoMM-2007-126

MODELING OF A CLAMPED-CLAMPED CARBON NANO-TUBE FLEXURAL ELEMENT FOR USE IN NANOELECTRO-MECHANICAL SYSTEMS

Michael Cullinan[1], Christopher DiBiasio[1], Larry Howell[2], Martin Culpepper[1*], and Robert Panas[1]
[1] Department of Mechanical Engineering, Massachusetts Institute of Technology,
Cambridge, Massachusetts, USA
[2] Department of Mechanical Engineering, Brigham Young University, Provo, Utah, USA

[*] Corresponding author (email: Culpepper@mit.edu)

Abstract

In this paper, we (1) present observations of the large-displacement behavior of a clamped-clamped carbon nanotube (CNT) flexure element and (2) provide an overview of a new pseudo-rigid-body (PRB) model that predicts its elastomechanic behavior. We also show how this element may be combined with others to create a flexure bearing that can guide motions in nanoelectromechanical systems. The mechanical properties of CNTs make it possible for CNT-based devices to achieve high bandwidth (e.g. 10s of GHz) and large motion ranges that will enable exciting applications in nano-scale instrumentation and metrology. Unfortunately, this compliant element experiences strain stiffening that leads to localized bending deformations in the CNT. As such, linearized macro-scale elastomechanic models fail to accurately predict the static response of the beam. Molecular simulations were used to make observations on the device's behavior and to extract its elastomechanic response. A PRB model for the new behavior was then created and its predictions were shown to match molecular simulation results with less than 13% deviation. This paper provides an understanding of (i) why this flexural element exhibits its unique behavior and (ii) how to model/make use of this behavior. The understanding and engineering models that are contained within this paper may be used to tailor the function of CNT-based flexures without the need to iterate with intensive molecular simulations. The work is in a nascent stage; however the results are an important pre-cursor to the realization of flexure-based nano-electro-mechanical systems.

Keywords: Carbon nanotube, Compliant mechanism, Flexure bearing

1 Introduction

This paper provides an overview of the modeling and design of a clamped-clamped carbon nanotube (CNT) flexural element. Single-walled carbon nanotubes (SWCNTs) are single molecules of carbon that may be visualized as a sheet of carbon atoms, which is known as graphene, that has been wrapped into a cylinder. The nature of the aromatic atomic bonds that are found in the SWCNT endow them with mechanical properties that are favorable to flexures. SWCNTs have been found to possess high strength (failure stress ~100 GPa [1]) and large failure strains (~40% [2]). These characteristics make it possible for CNT-based flexural devices to possess large bandwidths (e.g. 10s of GHz) and large motion ranges that will be useful in nanoelectromechanical devices. Unfortunately, this element experiences strain stiffening of such magnitude that conventional linear models do not accurately predict its elastomechanic behavior. The main focus of this paper is to explain why conventional models fail to predict the behavior with reasonable accuracy. We also report on nascent efforts to model this performance with a PRB model.

In short, the curvature of the tube's cross section is markedly different between the center of, and the end of, the beams. The zones of different deformation are shown in Fig. (1A).

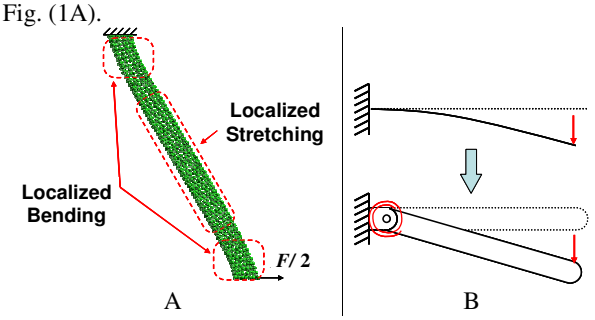

Figure 1: Deformations at the CNT's center and at its ends (A) and a PRB model of a flexural element (B)

Molecular simulations are capable of predicting the response of the flexure under these conditions. Unfortunately, accurate simulations may take days to complete for the analysis of a specific design. If one attempted to design a device that was (i) composed of several CNTs and (ii) required to possess specific stiffness requirements, several iterations of molecular simulations would be needed to ascertain the correct diameter to length ratios for the CNTs. Depending on the complexity of the problem, this simulation could take weeks or months. If one performs behavioral modeling with the PRB model it is pos-

sible to reduce the time to run this simulation to a few minutes.

In the past, we have shown that PRB model is well-suited to accurately predict the large, non-linear elastic bending of the compliant elements in a CNT-based device, for example a parallel guiding mechanism (nPGM) [3]. The PRB model is an elegant and accurate method that enables designers to model compliant mechanisms (CMs) as analogies to rigid-link mechanisms [4, 5]. The rigid analog's behavior is then modeled with conventional rigid mechanism theory. Figure (1B) shows a flexible cantilever and its PRB analog. Early work shows that the PRB model matches molecular simulation results with less than 13% difference, which is adequate for the purpose of rapidly setting initial design concept parameters. After an initial design is obtained, molecular simulations may be used, if desired, to obtain more accurate predictions.

2 Modeling, simulation, and observations

2.1 Molecular simulation of static deflection

Our molecular simulations modeled the static elastomechanic response of a clamped-clamped CNT beam that has a rigid stage mounted to the CNT at its midpoint. This was accomplished by applying specific boundary conditions to the ends of two coaxial (5,5) CNTs. The opposing ends of the CNTs beam were fixed in order to emulate a rigid CNT-substrate bond. The adjacent ends of the CNTs had two boundary conditions applied to them: (1) the circular cross sections could not deform under load and (2) the adjacent ends of the CNTs had to remain parallel and a fixed distance of 7.64 nm from each other. The displacements of the inner ends were coupled together in order to simulate the presence of the rigid stage at the center of the CNT beam. The model is shown in Fig. (2).

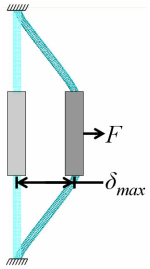

Figure 2: Molecular simulation model

A force, F, was applied in a direction that was perpendicular to the axis of the CNTs and along the lateral bisector of the clamped-clamped CNT. The CNTs were modeled as defect-free (5,5) single-walled CNTs (SWCNTs). We used defect-free tubes in order to provide a base line for future studies on the effect of defects within the CNT lattice. The individual tubes had a diameter of 0.678 nm and a length of 7.64 nm. The simulations utilized the MM+ force field. A Polak-Ribiere conjugate algorithm was used to minimize the energy of the system until the RMS gradient was less than 1 cal/Å mol.

Molecular simulations are difficult to set up, and they require days, or even weeks, to converge to an accurate solution. Given the match between the small-motion, cantilevered bending response of CNTs, and the predictions of beam bending equations [6] and shell theory [7], it would seem likely that a solid mechanics model could be used to predict the element's behavior. The large-deflection model, shown in Eq. (1) [8], is often used to predict the strain stiffening of macro-scale elastic beams when the length of the neutral axis is increased during deformation. Eq. (1) relates the applied force to the displacement of the center of the beam, δ_{max}, via the clamped-clamped beam length, L, flexural rigidity, $(EI)_{bending}$, and $(EA)_{axial}$. Eq. (2) gives the displacement profile of the beam, y, as a function of the axial position along the beam, x.

$$F = \frac{2\pi^4}{L^3}(EI)_{bend}\,\delta_{\max} + \frac{\pi^4}{8L^3}(EA)_{axial}\,\delta_{\max}^3 \tag{1}$$

$$y = \frac{\delta_{\max}}{2}\left(1+\cos\frac{2\pi x}{L}\right) \tag{2}$$

The simulated static response of the clamped-clamped CNT beam is plotted against the large-deflection model predictions as shown in Fig. (3). The geometry and material property values that are used within Eq. (1) were selected based upon established elastic moduli for different loading conditions and assumed wall thicknesses [9]. Figure (3) shows that the large-displacement solid mechanics model over-predicts the device stiffness by an amount that renders it useless for practical engineering modeling. The reason for the error may be understood by visually examining the shape of a deformed clamped-guided CNT beam as shown in Fig. (1A). The molecular simulations show localized bending in the CNTs at their anchoring points and axial deformation in the portion of the CNTs in between the bends. Eq. (1) provides an "upper bound" on the real behavior of the CNT-based device as it assumes that energy is required to bend the element throughout its entire length. From Fig. (1A), we observe that this is not true for the CNT at large deflections.

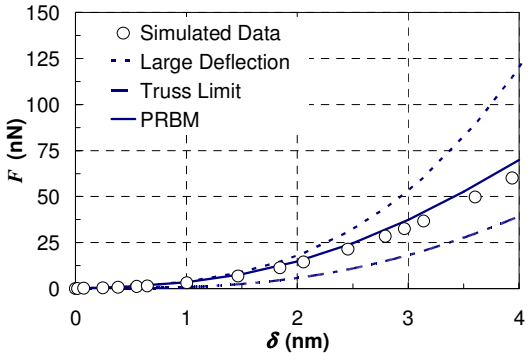

Figure 3. Elastomechanic response of the CNT-based clamped-clamped beam

A truss model was developed in order to provide a lower bound for the element's behavior. This model assumes that the CNTs are in pure axial tension and therefore it neglects the bending contributions at the end of the CNTs. This model will be used to provide insight into the nature of the deformation by showing that the magnitude of the device's stiffness is primarily due to axial stretching of the CNT that occurs at large displacements. The non-linear stiffness, k, of the beam for the truss model is given in Eq. (3).

$$k = \frac{(EA)_{axial} \sin^2\left[\tan^{-1}\left(\frac{\delta_{\max}}{L}\right)\right]}{\sqrt{L^2+\delta_{\max}^2}} \tag{3}$$

The predictions of Eq. (3) are plotted in Fig. (3). The truss model predicts the device stiffness with 64% error for deflections of less than 1 nm, where the bending stiffness constitutes the majority of the device's stiffness. For large deflections, this model exhibits 18% error versus the 91% that was obtained with the large deflection approach. This result suggests that the truss model may be augmented by using a PRB model [4], to accurately predict the combined bending and axial deformation response of the clamped-clamped beam. We will find that using a lumped parameter model such as the PRBM will eliminate the need to account for nano-scale phenomena such as van der Waals forces in our model. In contrast, a continuum mechanics formulation via Rayleigh-Ritz would require this addition.

2.2 Overview of the pseudo-rigid-body approach

Figure (4) shows one half of the CNT clamped-clamped compliant beam and its PRB mechanism equivalent.

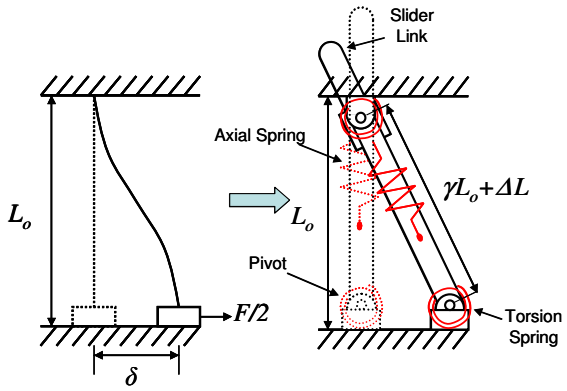

Figure 4: PRB model of a clamped-guided beam.

The rigid mechanism analog is created by using a characteristic radius factor, γ, to define the location of characteristic pivots that will cause the PRB mechanism to emulate the kinematics of the clamped-clamped beam. In our mechanism the pivots are located at a fixed position from the boundaries as defined by γ and the undeformed clamped-guided beam length, L_o. As the beam is deflected, the slider link between the two pivots is allowed to increase in length.

Torsion springs at the joints of the PRB mechanism make it possible to emulate the elastomechanic behavior of the CM. The torsional spring constant, K_T, is calculated as shown in Eq. (4), where K_θ is the stiffness coefficient.

$$K_T = 2 \cdot \frac{\gamma}{L_o} \cdot K_\theta \cdot (EI)_{bending} \tag{4}$$

A linear spring is also added to the slider link to counteract axial extension of the link during deformation. The axial spring constant, K_A, is calculated as shown in Eq. (5), where ΔL is the increase in slider link length.

$$K_A = \frac{(EA)_{axial}}{L_o + \Delta L} \tag{5}$$

The change in length of the slider link length is given in Eq. (6).

$$\Delta L = \sqrt{\delta_{\max}^2 + \gamma^2 L_o^2} - \gamma L_o \tag{6}$$

Results from the molecular simulations showed that a 6% reduction in cross-sectional area occurred as the CNT was axially loaded. This makes it necessary to relate the cross-sectional area with the increase in link length using Eq. (7).

$$A = \frac{\pi D_o L_o t\left[1+\frac{\Delta L}{L_o}(1-2\nu)\right]}{L_o + \Delta L} \tag{7}$$

In Eq. (7), D_o is the original CNT diameter, t is the assumed wall thickness of the CNT, and ν is the Poisson's ratio (0.28 [10] for SWCNT). The final force-displacement relationship given by the PRB model is shown in Eq. (8).

The principal of virtual work was used to correlate the element's displacement with its driving force, $F_{bearing}$.

$$F_{bearing} = 2K_A \Delta L \sin^{-1}\left(\frac{x}{\sqrt{x^2+\gamma^2 L_o^2}}\right) + \frac{4K_T \gamma L_o \tan^{-1}\left(\frac{x}{\gamma L_o}\right)}{x^2+\gamma^2 L_o^2} \tag{8}$$

The first term in Eq. (8) represents the component of the force vector that is associated with increasing the length of the slider link. The second term, which is dominated by the first term for large deformations, represents the lateral bending resistance of the CNT. Table 1 contains all the parameters used in our PRB model simulations:

Table 1: Parameters related to planar revolute joint

Variable	Value	Units
$(EA)_{axial}$	514.1	nN

$(EI)_{bending}$	35.68	$nN \cdot nm^2$
Γ	0.85	--
K_θ	2.65	rad^{-1}
L_o	7.64	nm
D_o	0.678	nm
t	0.075	Nm
ν	0.28	--

2.3 Pseudo-rigid-body model results

For displacements that are less than 1 nm, the large displacement beam bending model and PRB model both predict the stiffness of the clamped-clamped beam to within 10% of the simulated device stiffness. For displacements larger than 1 nm, the PRB model is more accurate than the large displacement beam bending model as can be seen in Fig. (3). The maximum error in the force estimates made by PRB model is less than 13%. In contrast, the large deflection models exhibit errors that exceed 90%. This implies that the localized bending assumption that was made within the PRB model is a more accurate representation of the flexure's behavior at large displacements.

While the PRB approach models the force-displacement relationship of the flexure with improved accuracy, the model is sensitive to the choice of the PRB parameter γ as shown in Fig. (5). For example, by changing γ from 0.85 to 0.91, the maximum error in the model may be reduced from 12.7% to 2.7%. The PRB model, however, is not overly sensitive to the choice of K_θ. This is due to the fact that for large displacements, over 90% of the deformation energy is stored via stretching the CNT. The value of K_θ contributes only to the bending term and not to the stretching term; therefore it does not have a large effect on the static response at large displacements. Overall, more experimental and theoretical work needs to be done in order to determine the exact pivot length of CNTs, i.e. to see if/how γ differs from the macro-scale value of 0.85.

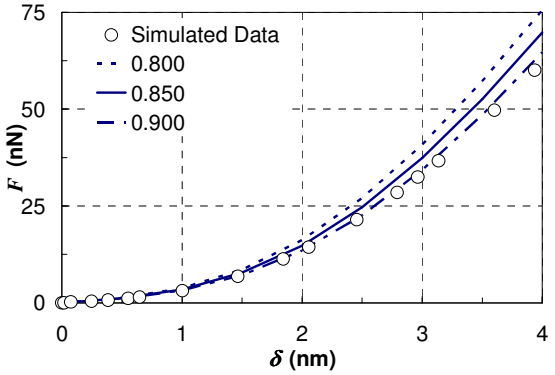

Figure 5: PRB model error as a function of γ

3 Example of practical utility

We now speculate on potential applications of nano-scale devices that may be realized by the incorporation of CNT-based clamped-clamped flexural beams. One example of a practical device that would utilize this flexural element is the flexure bearing that is shown in Fig. (6). Such a flexure could be made by laying down parallel CNTs down over a patterned substrate and using electron beam induced deposition of amorphous carbon or metal (using an SEM or FIB) in order to set the length of the flexure via the anchor points [12]. This type of bearing is a ubiquitous machine element that permits one rotational and two translational degrees-of-freedom. Our simulations show that a CNT-based bearing is capable of deformations that are 25% of its characteristic size. In contrast, a micro-scale silicon bearing of geometrically similar design would only be capable of deformations that are less than 1% of its characteristic size.

A promising application for this flexure bearing is high-speed precision motion control of probe tips that are used in metrology or nanomanufacturing. Given the preceding models, and the bearings they help to create, probes may be designed to improve the resolution and speed characteristics for scanning probe microscopy, or nano-electro-discharge machining systems. We are presently working to fabricate a device for the former application.

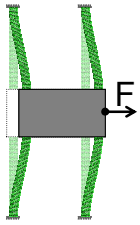

Figure 6: A CNT-based flexure bearing

Probe-based metrology methods, such as AFM, use probes that are attached to meso-scale cantilevers that are a few square millimeters in area. Probes that are placed upon CNT-based flexure bearings could be packaged into areas smaller than 10 square micrometers. As a result, thousands of CNT-based probes could be fit into the same area as a single conventional probe, thereby markedly increasing the number of measurements that could be made in a single scan pass. This correlates to decreasing the time that is required to measure surface topographies.

Another advantage of the CNT-based probing flexure bearings is that they possess higher natural frequencies than the meso-scale, cantilever-based probes. The cantilever-based probes typically operate in the 100s of kHz range while the CNT-based probes could operate over 1 GHz. This difference in natural frequency is due to (1) the boundary conditions of flexures used to guide the motion of the probes, i.e. cantilevered vs. doubly clamped, (2) the reduced mass of the system due to the reduction in size, and (3) the relatively high modulus/stiffness of the CNT based device verses silicon. Increasing the natural frequency, would enable faster response to commanded displacements and this would improve the flexure's disturbance rejection characteristics.

The high packing density of the CNT-based flexure bearings may also be useful for nanomanufacturing applica-

tions such as nano-EDM where the height of the electrode above the surface would be controlled by the flexure bearing. The high packing density should allow a large number of features to be written in a small area with high accuracy. The nano-scale bearings require less force to actuate than the macro-scale bearings typically used in EDM.

4 Conclusions

In this paper we have provided an explanation of (i) why a clamped-clamped flexural CNT element exhibits its unique behavior and (ii) how to model/make use of this behavior. The understanding and engineering models that are contained within this paper may be used to tailor the function of CNT-based flexures without the need to iterate with intensive molecular simulations. Molecular mechanics simulations of a clamped-clamped CNT beam have shown that the beam is capable of deformations of up to 25% of its length. For deformations larger than 1 nm, which is about 7% of the beam length, the CNT begins to exhibit localized bending and stretching deformation. These localized deformations make the behavior of the clamped-clamped CNT beam differ from the distributed bending behavior that is assumed for the macro-scale clamped-clamped beams.

A PRB model for the new behavior was created and its predictions were shown to match molecular simulation results with less than 13% error. The work is in a nascent stage; however the results are an important pre-cursor to the realization of flexure-based nano-electro-mechanical systems. For example, with additional work the PRB model could be used to design high-speed CNT-based probes for nano-manufacturing or metrology. Also, the PRB model may be used to design nano-scale actuators and sensors with large ranges of up to 25% of the device's characteristic length.

References

[1] S. Iijima, "Structural Flexibility of Carbon Nanotubes," Nature, Vol. 104, No. 5, 1991, pp. 2089-2092.

[2] J. Lu and L. Zhang, "Analysis of localized failure of single–wall carbon nanotubes," Comp. Mat. Sci., Vol. 35, 2006, pp 432–441.

[3] C.M. DiBiasio, M.L. Culpepper, R.M. Panas, L.L. Howell, and S. Magelby, "Comparison of Molecular Simulation and Psuedo-Rigid-Body Model Predictions for a Carbon Nanotube-based Compliant Parallel-guiding Mechanism," Under Review, Journal of Mechanical Design.

[4] L. L. Howell, Compliant Mechanisms, Wiley, New York, 2001.

[5] L. L. Howell and A. Midha "Parametric deflection approximations for end–loaded, large–deflection beams incompliant mechanisms," J. Mech Design, Vol. 117, 1995, pp. 156–165.

[6] C. Li and T. Chou, "A Structural Mechanics Approach to for the Analysis of Carbon Nanotubes" International Journal of Solids and Structures, Vol. 40, 2003, pp. 2487-2499.

[7] A. Pantano, D. Parks, and M. Boyce, "Mechanics of deformation of single- and multi-wall carbon nanotubes," Journal of the Mechanics and Physics of Solids, Vol. 52, 2004, pp. 789-821.

[8] S. Senturia, Microsystem Design, Kluwer Academic Publishers, Boca Raton, 2002.

[9] C. DiBiasio, M. Cullinan, and M. Culpepper, "The Difference Between Bending and Stretching Moduli of Single-Walled Carbon Nanotubes Modeled as an Elastic Tube," App. Phys. Lett., Vol. 90, No. 20, 2007, pp. 203116-203119.

[10] J.P. Lu, "Elastic Properties of Carbon Nanotubes and Nanoropes," Phys. Rev. Lett. Vol. 79, 1997, pp. 1297-1300.

[11] M. F. Yu, B. Files, S. Arepalli, and R. Ruoff, "Tensile loading of ropes of single wall carbon Nanotubes and their mechanical properties", Physical Review Letters, Vol. 84, No. 24, 2000, pp. 5552-5555.

[12] K. Molhave, D.N. Madsen, S. Dohn, and P. Boggild, "Constructing, connecting and soldering nanostructures by environmental electron beam deposition", Nanotechnology, Vol. 15, 2004, pp. 1047-1053.